

## Effects of Inter-Turbines Spacing on Aerodynamics for Wind Farms Based on Actuator Line Model

Yong Ai<sup>1</sup>, Decheng Wan<sup>1\*</sup>, Changhong Hu<sup>2</sup>

<sup>1</sup> Collaborative Innovation Center for Advanced Ship and Deep-Sea Exploration, State Key Laboratory of Ocean Engineering, School of Naval Architecture, Ocean and Civil Engineering, Shanghai Jiao Tong University, Shanghai, China

<sup>2</sup> Research Institute for Applied Mechanics, Kyushu University, Fukuoka, Japan

\*Corresponding author

### ABSTRACT

Among several wind farm layout design parameters, the inter-turbine spacing, which has a great influence on aerodynamic power output, wind speed deficit, lifetime, wake vortex structure, is one of the most critical factors. Therefore, the effects of inter-turbine spacing on aerodynamics for wind farms must be carefully studied. In this study, Considering the uniform inflow conditions, the effects of inter-turbine spacing changing from three to nine times of rotor diameter on aerodynamics for wind farms containing two NREL 5MW baseline wind turbines in tandem layout are analyzed using actuator line model and CFD method, and the RANS equation with  $k-\omega$  SST turbulence model was solved in the simulations conducted in the OpenFOAM. From the study, it is concluded that the inter-turbine spacing has significant effects on the aerodynamic power and wake characteristics. The aerodynamic power output of the downstream wind turbine exits sharp fluctuation before power output of the downstream wind turbine is becoming steady. Furthermore, periodic oscillation whose period is about the one-third of rotor rotating period can be also concluded from the study. Moreover, there is strong wake interaction which will impact the aerodynamics for wind farms seriously.

**KEY WORDS:** wind farm; actuator line model; CFD; aerodynamic power output; wake characteristics.

### INTRODUCTION

Wind energy is a promising renewable energy resource to help handle the environmental pollution caused by the extended use of fossil fuel. Wind farms, which have large capacity to contain plenty of wind turbines, are becoming the main electrical energy source. Since the broader application of wind energy, the layout design of wind farm is becoming significant (Chio, 2014). The layout design of wind farms that affects the initial investment cost, annual energy production, operation and maintenance cost during the service lifetime of wind turbines is a key factor (Kusiak, 2010). Among several wind farm layout design parameters, the inter-turbine spacing, which has a great

influence on aerodynamic power output, wind speed deficit, lifetime, wake vortex structure, is one of the most critical factors. We can know that, if the distance between two turbines is too small, there will be seriously effects on downstream turbines due to the strong wake interference, which will cause immeasurable drop of power output and stand higher loads on turbines experiencing wakes compared to those experiencing free stream flows (Barthelmie, 2009). Therefore, the effects of inter-turbines spacing on aerodynamics for wind farms must be carefully considered to fully study the aerodynamic power out, the wake characteristics and axial speed deficit, specially the wake interaction phenomenon.

In order to study the complex phenomenon existing in wind farms, lots of wake models were developed. Katic (1986) proposed a one-dimension wake model called Park wake model and applied it to the wind resource evaluating software named WAsP (*Wind Atlas Analysis and Application Programs*) (Mortensen et al., 2014). But the impact of turbulence intensity to the wake is neglected in this model. Faced with (Considering) the defect of Park wake model, Wang Feng (2010) improved the linear Park wake model into nonlinear wake model which is used in wind farm micro-sites selection research. Plenty of other wake models were latterly developed by other researchers, such as Ainslie wake model (Ainslie, 1988), Larsen wake model (Larsen, Hojstrup, Aagaard, 1996), which all belong to two-dimension wake model. And three-dimension wake models based on CFD theory were also proposed by some researchers, such as the RGU (*Robert Gordon University*) model which is 3-D Navier-Stokes numerical solver with  $k-\epsilon$  turbulence closure (Magnusson, 1996, Schlez, 2001). But a common disadvantage of these wake models is that they do not capture the actual turbulence characteristics in the wake, which may deviate significantly from that of the undisturbed flow field (Troldborg, 2011). It may cause that the wake interference on aerodynamics for the wind farm will be underestimated, which will lead to some incorrect and serious results. For example, we may not forecast accurately the aerodynamic loads which has close relationship with the fatigue problem on the blades. Some researchers also attempted to use wind tunnel experiment to study the wake vortex structure for a single turbine or wake interaction for wind farms. Whale, Anderson and Baireiss (2000) presented an experimental investigation into the

properties of the vortex behind a wind turbine rotor carried out at model scale, using Particle Image Velocimetry (PIV) technique. Vermeer (2003) studied the near wake and far wake for a single turbine and wind farms using wind tunnel experiment and presented several wake models for wind farm in near wake region and far wake region. Troldborg (2011) pointed out that, even though such studies provided useful information about some main features of the wake structure, they still put at a disadvantage due to the low Reynolds numbers and typical model scale effects. Obviously, it is unrealistic to use the experimental method to study the wake interaction for wind farms in full scale because of the high cost and long time period. Furthermore, Montavon and Jones (2009) found that CFD approach can be used to study wind farms with large advantage compared to experimental method by examining the use of CFD for the prediction of the wind power potential of a wind farm. His study showed good agreement with the measurements when being compared to data gathered during wind farm operation. Afterwards, Barthelme and Hansen (2009) have done a study focused on comparing different models from CFD to farm models in terms of how accurate the wake loss is presented when compared to measurements, which included that wind farm models need to be modified to reduce under-prediction while the CFD models typically over-predict wake loss. Chio (2013, 2014) presented the results of CFD simulations for a two turbine wind farm and a three turbine wind farm which both have the linear layout called tandem type and showed that the inter-turbine spacing parameter has significant effects on the aerodynamics for the wind farms, specially the aerodynamic power output. Considering that full three dimension CFD simulation for wind farm needs to generating mesh for the whole wind farm models including the rotor and boundary layer around blades, hub, nacelle, tower, which may take a long time to get final answers because of too large mesh number. A mixed method named actuator line model combined with CFD technique was developed by Sørensen and Shen (2002). A high-fidelity tool SOWFA (*Simulator fOr Wind Farm Applications*) (Churchfield and Lee, 2013), which is a LES framework coupled with FAST (*Fatigue, Aerodynamics, Structures, Turbulence*) (Jonkman, 2010), was used to analysis offshore wind turbine and wind farm based on that method. Troldborg and Larsen (2010) presented numerical simulations of wake interaction between two wind turbines at various inflow condition using actuator method coupled with EllipSys3D software (Michelsen, 1994; Sørensen, 1995). Churchfield, Lee and Moriarty (2012) have done a large-eddy simulation of the 48 multi-megawatt turbines composing the Lillgrund wind plant. Fleming, Gebraad and Lee (2015) presented a Simulation comparison of wake mitigation control strategies for a two-turbine case. Although there are already many studies using actuator line model to research the wake interactions for wind farms, there is still a great demand for more detailed and deep analysis for the wind farm until the nature of wake characteristics is entirely figured out.

This paper presents numerical simulations of a two turbine wind farm. Considering the inter-turbine Spacing, to research the aero-power output and power output ratio, wind speed deficit and wake characteristics using the actuator line model CFD technique to get some detail explanation for wake interaction according to the different inter-turbine spacing.

## NUMERICAL METHODS

### Actuator Line Model

The actuator line model (ALM) was firstly developed by Sørensen and Shen (2002). The rotating blades are virtualized into span wise sections of constant airfoil, chord and twist and the forces are distributed over them. Hence, there is not requirement to build the actual blades model.

Moreover, the lift force and drag force of each section can be calculated as:

$$L = \frac{1}{2} C_l(\alpha) \rho U_{rel}^2 c dr \quad (1)$$

$$D = \frac{1}{2} C_d(\alpha) \rho U_{rel}^2 c dr \quad (2)$$

Where,  $C_l$  and  $C_d$  are the lift and drag coefficient, respectively.  $\alpha$  is the attack angle,  $c$  is the chord length,  $U_{rel}$  is the local velocity relative to the rotating blade of each section.

In fig. 1 we can know that the local velocity relative to the rotating blade can be expressed as:

$$U_{rel} = \sqrt{U_z^2 + (\Omega r - U_\theta)^2} \quad (3)$$

There, the  $U_z$  and  $U_\theta$  are the axial velocity and tangential velocity, respectively. The  $\Omega$  is the rotor speed.

The attack angle is defined as:

$$\alpha = \phi - \gamma \quad (4)$$

Where, the  $\phi = \tan^{-1}(U_z / \Omega r - U_\theta)$  and the  $\gamma$  is the local pitch angle.

The body force  $f$  can be expressed as:

$$f = (L, D) = \frac{1}{2} \rho U_{rel}^2 c (C_l \bar{e}_L + C_d \bar{e}_D) \quad (5)$$

The applied aerodynamic blade forces need to be distributed smoothly on several mesh points in order to avoid singular behavior. In practice, a 3D Gaussian function is made to smooth the force over the blade by taking the convolution of the force with a regularization kernel,  $f_\varepsilon = f \otimes \eta_\varepsilon$ , where

$$\eta_\varepsilon(d) = \frac{1}{\varepsilon^2 \pi^{3/2}} \exp\left[-\left(\frac{d}{\varepsilon}\right)^2\right] \quad (6)$$

Here,  $d$  is the distance between cell-centered grid points and the  $i^{th}$  actuator line point, and  $\varepsilon$  is parameter that serves to adjust the concentration of the regularized loads.

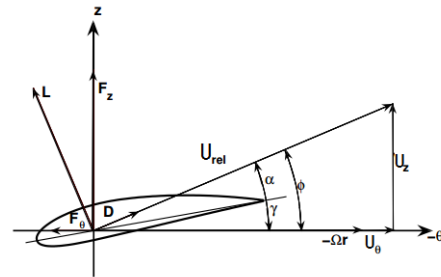


Fig. 1 Cross-sectional aero foil element (Sørensen and Shen, 2002)

### Governing Equation

In the present study, the RANS equation was solved, the expression can be written as:

$$\frac{\partial U}{\partial x_i} = 0 \quad (7)$$

$$\frac{\partial U_i}{\partial t} + \frac{\partial}{\partial x_j} (U_j U_i) = -\frac{1}{\rho} \frac{\partial p}{\partial x_i} + \frac{\partial}{\partial x_j} \left( \nu \frac{\partial U_i}{\partial x_j} - \overline{u_i' u_j'} \right) + \frac{1}{\rho} f \quad (8)$$

Where  $U$  is the velocity of flow;  $\rho$  is the density of the fluid;  $p$  is the pressure;  $\nu$  is the kinematic viscosity,  $f$  denotes the body forces, which represent the loading on the rotating blades. The body force acting on

the blades are determined using a blade element method combined with tabulated two-dimensional airfoil characteristics. The SST  $k-\omega$  turbulence model is applied to solved the RANS equation due to the closure problem, in which the turbulent kinetic energy  $k$  and the turbulent dissipation rate can be expressed as:

$$\frac{\partial}{\partial t}(\rho k) + \frac{\partial}{\partial x_i}(\rho k u_i) = \frac{\partial}{\partial x_j}(\Gamma_k \frac{\partial k}{\partial x_j}) + G_k - Y_k + S_k \quad (9)$$

$$\frac{\partial}{\partial t}(\rho \omega) + \frac{\partial}{\partial x_i}(\rho \omega u_i) = \frac{\partial}{\partial x_j}(\Gamma_\omega \frac{\partial \omega}{\partial x_j}) + G_\omega - Y_\omega + D_\omega + S_\omega \quad (10)$$

Where,  $\Gamma_k$  and  $\Gamma_\omega$  are the effective diffusion coefficients for the turbulent kinetic energy  $k$  and the turbulent dissipation rate  $\omega$  respectively,  $G_k$  and  $G_\omega$  are turbulence generation terms,  $Y_k$  and  $Y_\omega$  are turbulent dissipation terms,  $D_\omega$  is the cross-diffusion term for  $\omega$ ,  $S_k$  and  $S_\omega$  are the source term.

## SIMULATION SETUP

The wind farm contains two turbines which are all the NREL 5MW baseline wind turbines (Jonkman, 2009). Table 1 gives some specification of NREL 5MW baseline wind turbine used in this present study.

The wind farm layout is typical linear layout called tandem type. The distance of two turbines is changed to do the wind farm simulations. The detail arrangement is showed in Fig. 2.

Table 1. parameters of NREL-5MW turbine

Rating	5 MW
Rotor Orientation	Upwind
Number of blades	3
Rotor Diameter, Hub Diameter	126 m, 3 m
Hub Height	90 m
Cut-in, Rating, Cut-out	3 m/s, 11.4 m/s, 25 m/s
Cut-in, Rating Rotor Speed	6.9 rpm, 12.1 rpm
Overhang, Shaft Tilt, Precone Angles	5 m, $-5^\circ$ , $2.5^\circ$

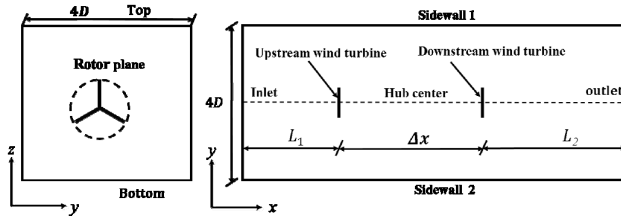
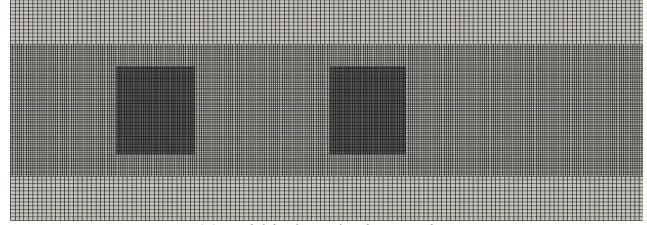


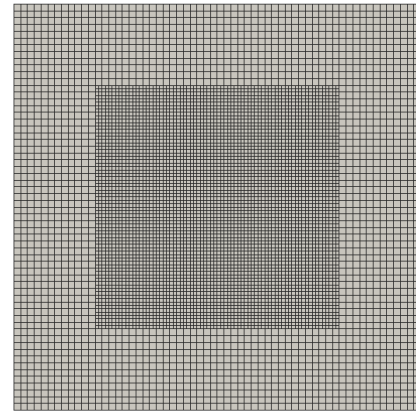
Fig. 2 wind farm arrangement

The computations are conducted in a Cartesian domain as sketched in Figure. 2, which also serves to define the used coordinate system. All distances are based on the rotor diameter  $D$  equal to 126 m. The height and width of the whole computational domain are kept in  $4D$ , respectively. the distance  $L_1$  from the inlet to the upstream wind turbine is kept in  $2D$ . In different simulation cases, the distance  $\Delta x$  and  $L_2$  which is the distance from downstream wind turbine to outlet are changed from  $3D$  to  $9D$  and  $8D$  to  $2D$ , respectively. Meanwhile, the height of hub for each wind turbine is kept in the same value equal to 90 m.

In order to resolve the strong gradients in the vicinity of the actuator lines, there are three parts in the mesh system. The first part is the outer mesh which is an initial mesh part for the whole flow field; from the Fig.3 (b), it can be figured out that the second part whose length is the same as the length of flow field and the height and width are  $2D$ , respectively, is the refinement mesh that has one level refinement based on the initial mesh in the entire computational domain grid. There are two fine mesh refinements whose refine level is two and length is  $1D$  and height and width are  $1.5D$  from Fig. 3(a), which aims to capture the near wake characteristics for each wind turbine, respectively. In order to control the total grid number is not too large, the far region of each wind turbine do not execute two level refinement any more. Finally, the total mesh was controlled about 3.6 million for each case.



(a) Grid in lengthwise section



(b) Grid in cross section

Fig.3 the grid in lengthwise section and cross section

All simulation cases are in the same uniform free-stream flow whose velocity is equal to the rated speed 11.4 m/s. the airfoil data of blades is prepared to be the interpolation database, which contains lift and drag coefficient, twist angle of each section in different airfoils. There are seven cases in which the parameter  $\Delta x$  and  $L_2$  are changed in different values in this present study to attempt to get some detail information about aerodynamic power output, axial speed deficit and wake interference. The detail information about each case is listed in Table 2.

In this study, the uniform free-stream flow condition whose values is 11.4 m/s at the reference height of hub is applied to the inlet defined in Fig. 2, respectively. A relative pressure of 0 Pa based on the atmospheric pressure is chosen for outlet boundary. Free-slip condition is applied to the top boundary, which means there is no wind speed gradient vertically and no flow across the top surface. Considering the bottom boundary as the sea surface, the no slip condition is applied to it and the sidewall 1 and sidewall 2 boundary are set to symmetry.

To ensure that the flow is fully developed in most of the wake, the computation duration is about 300 seconds. The computational time step is given to 0.005s to avoid the numerical divergence and more accurate numerical data could be obtained. Meanwhile, the parameter  $\varepsilon$  existed in Eq. 6 and named Gaussian width parameter, has a significant influence in the CFD simulation. this value of  $\varepsilon$  is roughly the minimum at which the force is smoothed enough to avoid spurious oscillations in the resulting velocity field using a central spatial discretization scheme (Churchfield, 2012). In this study, the parameter  $\varepsilon$  is kept to equal to twice the local grid size around blades (Martínez, 2012).

Table 2. simulation cases setup

Case Number	$\Delta x$	$L_2$	Remark
1	3D	8D	D=126 m
2	4D	7D	
3	5D	6D	
4	6D	5D	
5	7D	4D	
6	8D	3D	
7	9D	2D	

## RESULTS AND DISSCUSIONS

### Aerodynamic Power Output

From present study, the time history curves of aerodynamic power out for all cases are obtained. The time history curves of aerodynamic power output are showed in Fig. 4~10. To analyze the wake interaction on the aerodynamic power output of the downstream wind turbine, the results of upstream and downstream wind turbine in the same case are picked out.

From Fig. 4~10, the aerodynamic power outputs are steadier in a very short time of upstream wind turbine in all cases, rather than the downstream wind turbine, where sharp fluctuations exist in the aerodynamic power outputs which is conspicuous. After the fluctuations, the value of the power outputs is becoming steady in all cases, just like the power output of the upstream wind turbines. Furthermore, the appearing time of the fluctuation increases along with the increase of the parameter  $\Delta x$ . This curious phenomenon may result from that only the wake evolves a long distance after going across the downstream wind turbine can the flow is becoming to steady. It also can be figured out that the aerodynamic power outputs of upstream wind turbine nearly keep in the same value equal to 5.3 MW approximately from the present results. Inversely, there is obvious decrease in the aerodynamic power output of downstream wind turbine. the smaller the distance is between the upstream and downstream wind turbine, the more largely aerodynamic power output decreases. From the Fig. 4~10, this conclusion can be drawn lightly. This result implies a strong interaction between the upstream and downstream wind turbines in the wind farm which is designed as the typical linear layout called tandem type. As Choi (2013) pointed out that, in theory, a complete recovery of the downstream wind turbine's power output requires infinite separation distance between wind turbines, we can believe that there will be strong interaction between upstream and downstream wind turbine on their power output. Moreover, when the inter-turbine spacing is in a very small distance, the interaction will be stronger, which may have bad influence to the whole farm power output and lifetime.

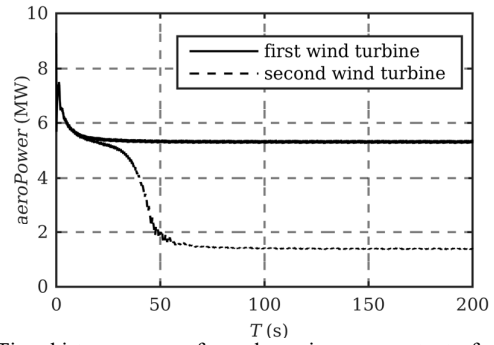


Fig. 4 Time history curves of aerodynamic power output of upstream and downstream wind turbine in case 1 ( $\Delta x = 3D$ )

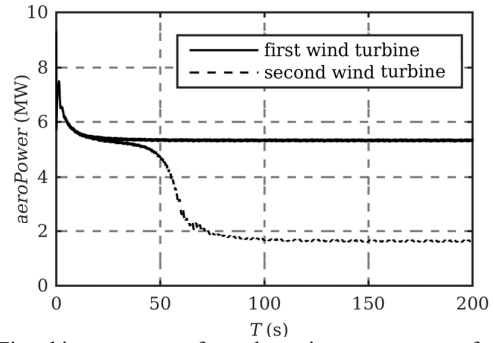


Fig. 5 Time history curves of aerodynamic power output of upstream and downstream wind turbine in case 2 ( $\Delta x = 4D$ )

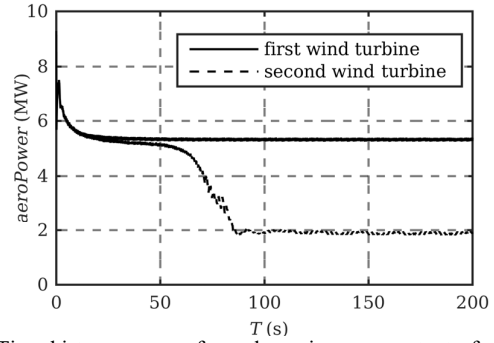


Fig. 6 Time history curves of aerodynamic power output of upstream and downstream wind turbine in case 3 ( $\Delta x = 5D$ )

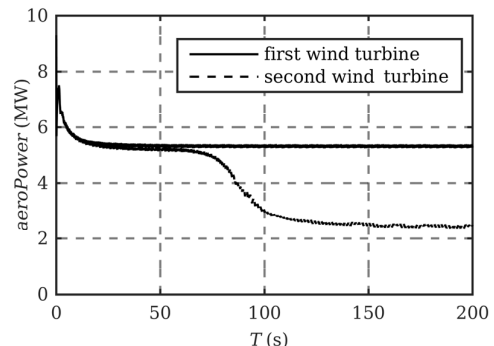


Fig. 7 Time history curves of aerodynamic power output of upstream and downstream wind turbine in case 4 ( $\Delta x = 6D$ )

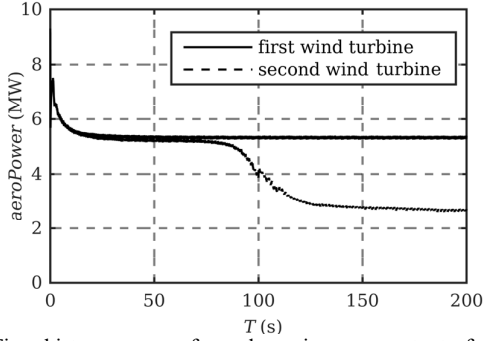


Fig. 8 Time history curves of aerodynamic power output of upstream and downstream wind turbine in case 5 ( $\Delta x = 7D$ )

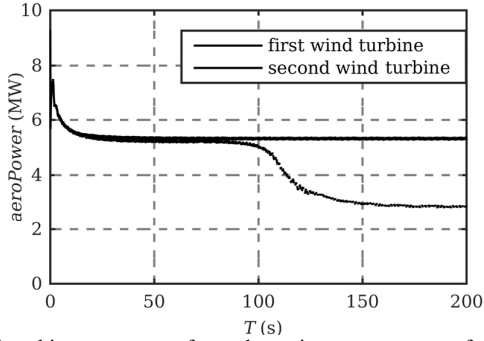


Fig.9 Time history curves of aerodynamic power output of upstream and downstream wind turbine in case 6 ( $\Delta x = 8D$ )

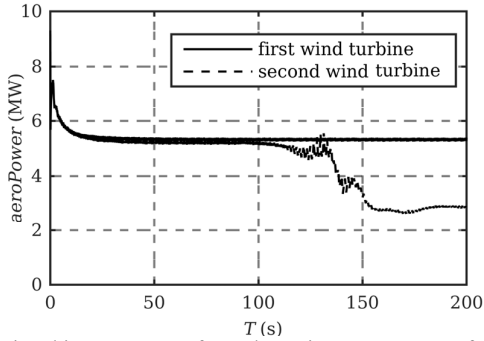


Fig. 10 Time history curves of aerodynamic power output of upstream and downstream wind turbine in case 7 ( $\Delta x = 9D$ )

Fig. 11 shows that the Time history curves of aerodynamic power output of downstream wind turbine after enlarging the initial time history curves in a same duration in case 5~7 ( $\Delta x = 7D, 8D, 9D$ ). From the figure, clearly view can be seen that there is obvious oscillation respect to the time of the downstream wind turbine, which is (a) periodic variation that the oscillation of period equals to one-third period of rotor rotating period roughly whose values is about 4.96 seconds and some similar results are also appeared in the rest cases. The reason of this interesting phenomenon may be that the tip vortex shedding of each blade of the upstream wind turbine is periodic, so the tip vortex shedding from each blade will have a strong interaction to the downstream wind turbine, which will have significant impact on the aerodynamic power output with respect to the simulation time. Meanwhile, the NREL 5MW baseline wind turbine we use in the wind farm simulation contains 3 blades, so there is no doubt that the tip

vortex shedding period is one-third period of rotor rotating. Furthermore, the rotor speed of the NREL 5MW baseline wind turbine equals to 12.1 rpm. The value of its period can be calculated out about 4.96 seconds through the simple mathematical relationship between the rotor speed and rotating period, this is why the oscillating period of aerodynamic power output of downstream wind turbine is equal to 1.66 seconds, roughly. From the results and discussion, it can be concluded that there is strong interaction of the wake from the upstream wind turbine to the downstream wind turbine, and the interaction will be changed with respect to the inter-turbine spacing.

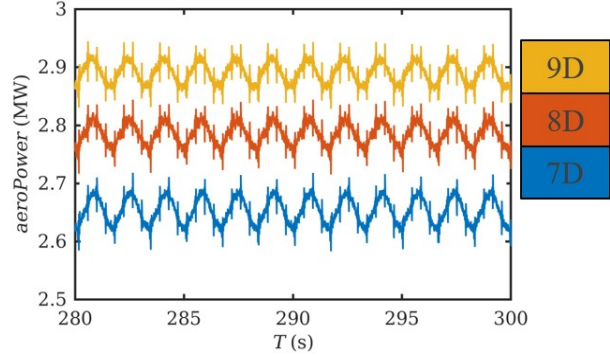


Fig. 11 Time history curves of aerodynamic power output of downstream wind turbine after enlarging the initial time history curves in case 5~7 ( $\Delta x = 7D, 8D, 9D$ ).

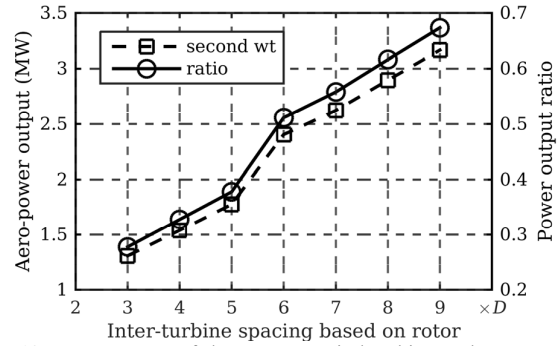


Fig. 12 Power output of downstream wind turbine and power output ratio.

Fig. 12 shows the aerodynamic power output of downstream wind turbine and power output ratio which can be defined as:

$$\text{power output ratio} = \frac{\text{power out of downstream wind turbine}}{\text{power out of upstream wind turbine}} \quad (11)$$

From Fig. 12, it is obvious that the aerodynamic power output of downstream wind turbine is changed with respect to the inter-turbine spacing between wind turbines. This result implies a strong interaction between the upstream and downstream wind turbines in the wind farm which is designed as the typical linear layout called tandem type. In previous analysis, it can be concluded that, there is weakened effects of downstream wind turbine on upstream wind turbine. Nevertheless, the aerodynamic power output of downstream wind turbine changes significantly with respect to the distance between upstream and downstream wind turbines. When the downstream is completely close to the upstream wind turbine, such as the case 3, which only has a distance in  $3D$  between the upstream and downstream wind turbines,

the power ratio is only about 26.15 percentages. Thus, there is great power loss of the downstream wind turbine owing to the strong wake influence from the upstream wind turbine. As the distance is increased from  $3D$  to  $5D$ , it can be easily concluded that the power output of downstream wind turbine increases gradually but very slowly at the same time. This main reason is may that the axial speed of flow behind the upstream wind turbine recovers little by little when the inter-turbine spacing is raised from  $3D$  to  $5D$ , whereas, the downstream wind turbine still located in the strong wake region from the upstream wind turbine, which impedes the increasing of the axial direction's speed. Due to the reason, the speed has recovered incompletely. With the distance increasing to  $6D$ , there is an obviously increase of power output compared to the power output of downstream located in  $5D$ . Quick increase appears when downstream wind turbine is located in  $7D$ ,  $8D$  and  $9D$  due to the weak wake interference from the upstream wind turbine. Owing to the weak wake influence, the axial direct speed of flow recovers quickly and almost fully, the down-stream wind turbine can output larger aerodynamic power.

In a word, from the present results of Fig.12, it can be concluded that when the downstream wind turbine is located near the upstream wind turbine, there will be a strong wake influence region which may cause less power output of downstream wind turbine in a wind farm whose layout is a tandem style. furthermore, equivalent to the strong wake region, there is also a weak wake region in the farm flow region. when downstream wind turbine is located in this region, there will be appreciable increase along with the inter-turbine distance increase. Fig. 12 also shows that there is a nonlinear relationship of power output ratio with respect to the distance between upstream and downstream wind turbines. The characteristics of power output ratio variation can also give enough proofs to support above conclusions. Just like Chio (2013) figured out that the wave length from the upstream wind turbine was almost constant, but the location of the downstream wind turbine could be inside or outside the strong wake region according to the separation distance. When the downstream wind turbine was placed in the strong wake region of the upstream wind turbine, the power output of the downstream wind turbine decreased due to the reduced incident wind speed compared to the upstream wind speed (Ole Rathmann et al., 2012).

### Wake Characteristics

It shows the profiles of the streamwise velocity in horizontal plane through the center of wind turbine rotor for case 1-7 in Fig. 13~19, respectively. Troldborg (2012) in his study figured out that the transition of the mean velocity profile, initially reflecting the rotor thrust distribution, into a bell-shaped form and subsequent recovery

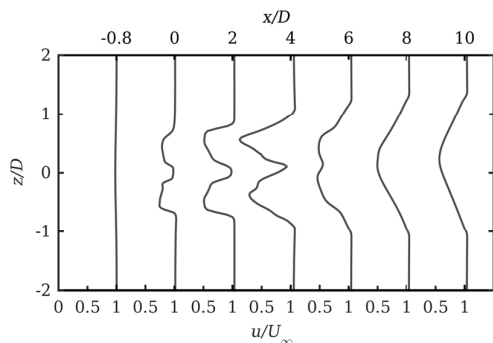


Fig. 13 Profiles of the streamwise velocity in horizontal plane through the center of wind turbine rotor for case 1.

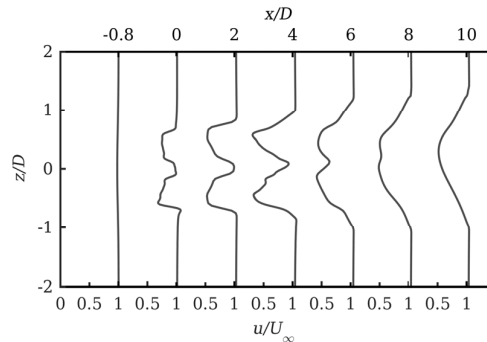


Fig. 14 Profiles of the streamwise velocity in horizontal plane through the center of wind turbine rotor for case 2.

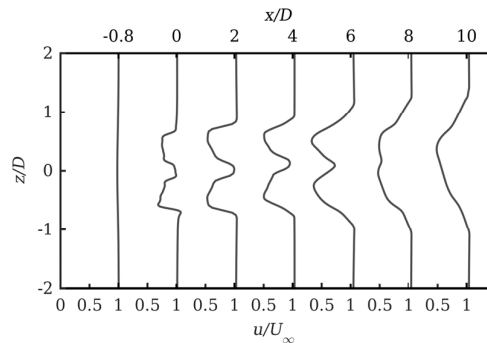


Fig. 15 Profiles of the streamwise velocity in horizontal plane through the center of wind turbine rotor for case 3.

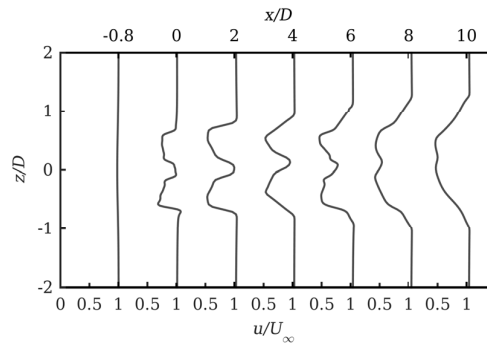


Fig. 16 Profiles of the streamwise velocity in horizontal plane through the center of wind turbine rotor for case 4.

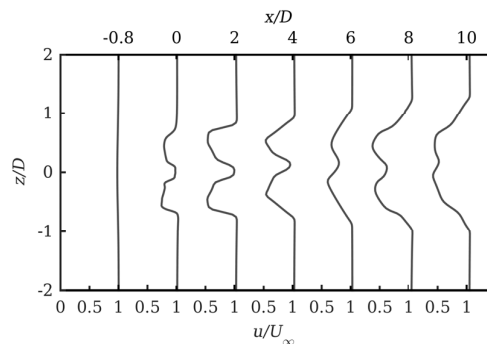


Fig. 17 Profiles of the streamwise velocity in horizontal plane through the center of wind turbine rotor for case 5.

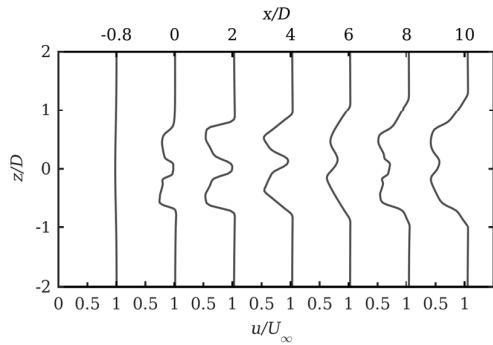


Fig. 18 Profiles of the streamwise velocity in horizontal plane through the center of wind turbine rotor for case 6.

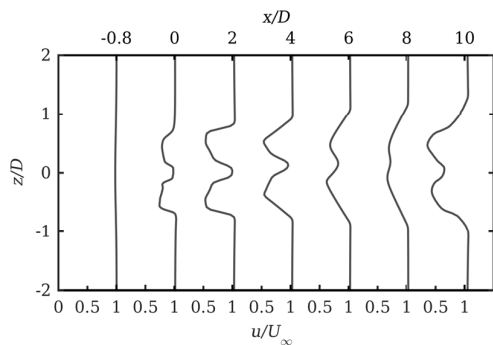


Fig. 19 Profiles of the streamwise velocity in horizontal plane through the center of wind turbine rotor for case 7.

occurs faster with increasing ambient turbulence. it can be clearly concluded that there are obvious changes of the speed in the wake of the upstream wind turbines. Two peaks pointing to the left and only one to the right.

Peaks pointing to left represent the speed decreases and the right peak means speed recovery. when the upstream and downstream wind turbines are in a close distance, there is strong wake interference which may be the main reason that causes the serious change in velocity of wake flow in case 1~3 (see in table 2), in which the distance is  $3D$ ,  $4D$  and  $5D$  between upstream and downstream wind turbines, respectively. When that distance is less than  $5D$ , the wake region is regarded as strong wake interaction region. Meanwhile, the speed is recovered gradually at the far wake region with different distance in different cases and the distance of speed recovery is about  $10D$  in cases 1~3, considering the wake interference of the upstream and downstream wind turbines. It also can be found that there are speed decreases in a long distance in cases 4~6 in which the distance is  $6D$ ,  $7D$  and  $8D$ , it implies that the wake influence of upstream wind turbine is strong and in a long distance. In these cases, there is still obvious wake interaction. From Fig. 19, it can be roughly figured out that the longest distance of wake influence of upstream wind turbine is about  $8D$ , for the reason that the rotor rotating effects and vortex shedding effects become weakest in this case.

These results can also give a reasonable explanation why the power outputs of downstream wind turbine increase slowly when the distances increase. When the two wind turbines get closer to each other, obvious decrease in axial velocity appears and the recovery of axial velocity is quite slow, resulting in severe power loss for downstream wind turbine.

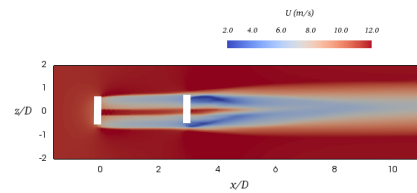


Fig. 20 Wind speed contour at hub height for case 1 in axial direction.

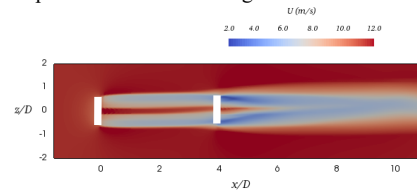


Fig. 21 Wind speed contour at hub height for case 2 in axial direction.

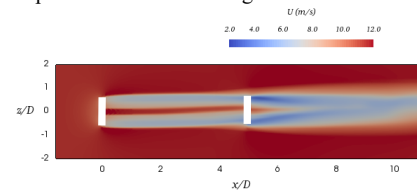


Fig. 22 Wind speed contour at hub height for case 3 in axial direction.

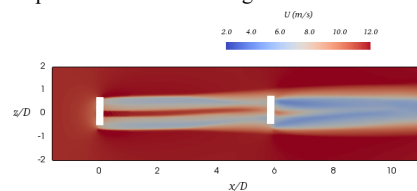


Fig. 23 Wind speed contour at hub height for case 4 in axial direction.

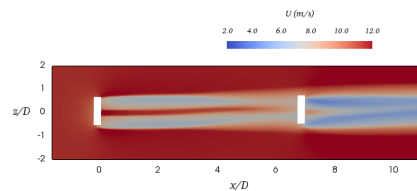


Fig. 24 Wind speed contour at hub height for case 5 in axial direction.

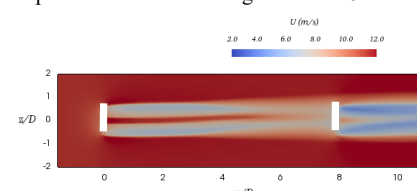


Fig. 25 Wind speed contour at hub height for case 6 in axial direction.

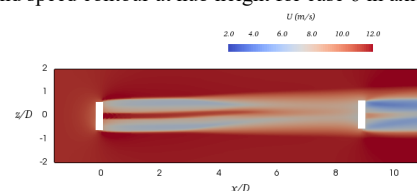


Fig. 26 Wind speed contour at hub height for case 7 in axial direction.

The wind speed at hub height for case 1~7 is shown in Fig. 20~26,



respectively. Obvious wake effects and interference is clearly identified. In case 3, Owing to the too closely distance between two turbines, sharp decrease of the speed of flow. Similar conclusions are also found

in the case 4~5 since the downstream wind turbine is located at the strong wake region. When the place of the second wind turbine is out of the strong wake region the wake effects is weak and the speed recovers gradually. As a results, increases in power output of downstream wind turbine is occurred. The phenomenon of the wake expansion can be clear observed in all cases. Furthermore, owing to the wake interaction of two turbines, the radius of wake expansion is bigger than the single wind turbines comparing to the case1 and 7.

## CONCLUSIONS

Considering uniform inflow condition, a numerical study of the effects of inter-turbines spacing changed from three to nine times of rotor diameter on aerodynamics for wind farms contained two NREL 5MW baseline wind turbines in tandem layout are analyzed successful using actuator line model and CFD technique, and the RANS equation with  $k-\omega$  SST turbulence model was solved in the simulations conducted in the OpenFOAM. From this analysis, it can be found that the inter-turbines spacing is a crucial factor in the wind farm layout design, which may have significant influence on the aerodynamics of wind turbine, specially the aerodynamic power output. First, sharp fluctuations exist in the aerodynamic power outputs of downstream wind turbine. After the fluctuations, the value of the power outputs becomes steady. Furthermore, the appearing time of the fluctuation increases along with the increase of the parameter, the inter-turbines spacing. Obvious and periodic oscillation whose period is about one-third rotor rotating period is concluded from the study. Third, the power output of downstream wind turbine was changed from about 26% to 68% compared to that of the upstream wind turbine as the separation distance was changed from 3D to 9D. A nonlinear relationship between the power output of downstream wind turbine and the non-dimensional separation distance can be also implied from the present results. When the distance between up and downstream wind turbines is less than 5D, the wake region is regarded as strong wake interaction region in which the flow speed will recover slowly. Hence, the distance 5D can be regarded as the design criterion for the wind farm design when the layout is tandem.

Although there are already many studies using actuator line model to research the wake interactions for wind farms, there is still (a) great demand for more detail and deep analysis for the wind farm until the nature of wake characteristics is entirely figured out. In the future work, the impact of the turbulent inflow, inflow speed below rated speed can be fully considered to study the aerodynamics of windfarms. Furthermore, the LES simulation can also be used to researched the wake interaction to get more useful information for the wind farm.

## ACKNOWLEDGEMENTS

This work is supported by the National Natural Science Foundation of China (51379125, 51490675, 11432009, 51579145), Chang Jiang Scholars Program (T2014099), Shanghai Excellent Academic Leaders Program (17XD1402300), Shanghai Key Laboratory of Marine Engineering (K2015-11), Program for Professor of Special Appointment (Eastern Scholar) at Shanghai Institutions of Higher Learning (2013022), Innovative Special Project of Numerical Tank of Ministry of Industry and Information Technology of China(2016-23/09) and Lloyd's Register Foundation for doctoral student, to which the authors are most grateful.

## REFERENCES

- Ainslie, J. F. (1988). Calculating the flowfield in the wake of wind turbines. *Journal of Wind Engineering and Industrial Aerodynamics*, 27(1), 213-224.
- Bachant, P., & Wosnik, M. (2016). Modeling the near-wake of a vertical-axis cross-flow turbine with 2-D and 3-D RANS. *arXiv preprint arXiv:1604.02611*.
- Barthelmie R J, Hansen K, Frandsen S T, et al. (2009). Modelling and measuring flow and wind turbine wakes in large wind farms offshore[J]. *Wind Energy*, 12(5): 431-444.
- Barthelmie, R. J., Pryor, S. C., Frandsen, S. T., Hansen, K. S., Schepers, J. G., Rados, K., ... & Neckelmann, S. (2010). Quantifying the impact of wind turbine wakes on power output at offshore wind farms. *Journal of Atmospheric and Oceanic Technology*, 27(8), 1302-1317.
- Cheng, P., Wan, DC (2015). Numerical Simulations of Complex Aerodynamic Flows around NREL Offshore 5-MW Baseline Wind Turbine[C]. *Proceedings of the 9th International Workshop on Ship and Marine Hydrodynamics(IWSH 2015)*, Glasgow, UK.
- Cheng, P., Wan, DC, & Hu, C. (2016, June). Unsteady Aerodynamic Simulations of Floating Offshore Wind Turbines with Overset Grid Technology. *Proc 26th Int Offshore and Polar Eng Conf*, Rhodes, ISOPE, 391-398.
- Choi, N. J., Nam, S. H., Jeong, J. H., & Kim, K. C. (2013). Numerical study on the horizontal axis turbines arrangement in a wind farm: Effect of separation distance on the turbine aerodynamic power output. *Journal of Wind Engineering and Industrial Aerodynamics*, 117, 11-17.
- Choi, N. J., Nam, S. H., Jeong, J. H., & Kim, K. C. (2014). CFD Study on Aerodynamic Power Output Changes with Inter-Turbine Spacing Variation for a 6 MW Offshore Wind Farm. *Energies*, 7(11), 7483-7498.
- Churchfield, M. J., Lee, S., Michalakes, J., & Moriarty, P. J. (2012). A numerical study of the effects of atmospheric and wake turbulence on wind turbine dynamics. *Journal of turbulence*, (13), N14.
- Churchfield, M. J., Lee, S., Moriarty, P. J., Martinez, L. A., Leonardi, S., Vijayakumar, G., & Brasseur, J. G. (2012). A large-eddy simulation of wind-plant aerodynamics. *AIAA paper*, 537, 2012.
- Churchfield, M., & Lee, S. *NWTC design codes* (SOWFA), 2013.
- Fleming, P., Gebraad, P. M., Lee, S., Van Wingerden, J., Johnson, K. E., Churchfield, M. J., ... & Moriarty, P. (2015). Simulation comparison of wake mitigation control strategies for a two-turbine case. *Wind Energy*, 18(12), 2135-2143.
- Hernandez, W., López-Presa, J. L., & Maldonado-Correa, J. L. (2016). Power Performance Verification of a Wind Farm Using the Friedman's Test. *Sensors* (Basel, Switzerland), 16(6),816. <http://doi.org/10.3390/s16060816>
- Jonkman, J. (2010). NWTC design codes (FAST). <https://mwtc.nrel.gov/FAST>.
- Katic, I., Højstrup, J., & Jensen, N. O. (1987). A Simple Model for Cluster Efficiency. In W. Palz, & E. Sesto (Eds.), *EWEC'86. Proceedings. Vol. 1* (pp. 407-410). Rome: A. Raguzzi.
- Kiranoudis, C. T., Voros, N. G., & Maroulis, Z. B. (2001). Short-cut design of wind farms. *Energy Policy*, 29(7), 567-578.
- Kusiak, A., & Song, Z. (2010). Design of wind farm layout for maximum wind energy capture. *Renewable Energy*, 35(3), 685-694.
- Langhamer, O., Holand, H., & Rosenqvist, G. (2016). Effects of an Offshore Wind Farm (OWF) on the Common Shore Crab *Carcinus maenas*: Tagging Pilot Experiments in the Lillgrund Offshore Wind Farm (Sweden). *PLoS one*, 11(10), e0165096.
- Larsen, G. C., Højstrup, J., & Madsen, H. A. (1996). Wind fields in wakes. In 1996 European Union wind energy conference. *Proceedings. HS Stephens & Associates*.
- Li, P, Cheng, P, Wan, DC (2015). Numerical Simulation of Wake Flows of Floating Wind Turbines by Unsteady Actuator Line



- Model[C]. *Proceedings of the 9th International Workshop on Ship and Marine Hydrodynamics (IWSH2015)*, Glasgow, UK.
- Li, P., Wan, DC, & Hu, C. (2016, June). Fully-Coupled Dynamic Response of a Semi-submerged Floating Wind Turbine System in Wind and Waves. *In The 26th International Ocean and Polar Engineering Conference. International Society of Offshore and Polar Engineers.*
- Magnusson, M., Rados, K. G., & Voutsinas, S. G. (1996). A study of the flow downstream of a wind turbine using measurements and simulations. *Wind Engineering*, 20(6).
- Michelsen, J. A. (1992). Basis3D-a platform for development of multiblock PDE solvers (pp. 92-05). *Technical Report AFM 92-05*, Technical University of Denmark.
- Michelsen, J. A. (1994). Block structured Multigrid solution of 2D and 3D elliptic PDE's. Department of Fluid Mechanics, Technical University of Denmark.
- Montavon, C. A., Jones, I. P., Staples, C., Strachan, C., & Gutierrez, I. (2009, March). Practical issues in the use of CFD for modelling wind farms. *In Proc European Wind Energy Conference.*
- Politis, E. S., Prospathopoulos, J., Cabezon, D., Hansen, K. S., Chaviaropoulos, P. K., & Barthelmie, R. J. (2012). Modeling wake effects in large wind farms in complex terrain: the problem, the methods and the issues. *Wind Energy*, 15(1), 161-182.
- Porté-Agel, F., Wu, Y. T., Lu, H., & Conzemi, R. J. (2011). Large-eddy simulation of atmospheric boundary layer flow through wind turbines and wind farms. *Journal of Wind Engineering and Industrial Aerodynamics*, 99(4), 154-168.
- Schlez, W., Umaña, A., Barthelmie, R., Larsen, G., Rados, K., Lange, B., ... & Hegberg, T. (2001). ENDOW: Improvement of wake models within offshore wind farms. *Wind Engineering*, 25(5), 281-287.
- Sørensen, J. N., & Shen, W. Z. (2002). Numerical modeling of wind turbine wakes. *Journal of fluids engineering*, 124(2), 393-399.
- Troldborg, N., Larsen, G. C., Madsen, H. A., Hansen, K. S., Sørensen, J. N., & Mikkelsen, R. (2011). Numerical simulations of wake interaction between two wind turbines at various inflow conditions. *Wind Energy*, 14(7), 859-876.
- Vermeer, L., Sørensen, J., & Crespo, A. (2003). Wind turbine wake aerodynamics. *Progress in Aerospace Sciences*, 39(6), 467-510.
- Wang, F (2010). wind sources evaluation for wind farm and optimization research of the layout [D]. Nanjing University
- Whale, J., Anderson, C. G., Bareiss, R., & Wagner, S. (2000). An experimental and numerical study of the vortex structure in the wake of a wind turbine. *J. Wind Eng. Ind. Aerodyn.* 84 (2000), 1-21
- Zhao, W, Cheng, P, Wan, DC (2014). Numerical Computation of Aerodynamic Performances of NREL Offshore 5-MW Baseline Wind Turbine[C]. *The Proceedings of the Eleventh (2014) Pacific/Asia Offshore Mechanics Symposium (PACOMS-2014)*, Shanghai, China, October 12-16, 2014, ISOPE, 13-18